

Cosmology-independent Estimate of the Hubble Constant and Spatial Curvature Using Time-delay Lenses and Quasars

JUN-JIE WEI^{1,2,3} AND FULVIO MELIA⁴¹*Purple Mountain Observatory, Chinese Academy of Sciences, Nanjing 210023, China*²*Guangxi Key Laboratory for Relativistic Astrophysics, Guangxi University, Nanning 530004, China*³*University of Chinese Academy of Sciences, Beijing 100049, China*⁴*Department of Physics, The Applied Math Program, and Department of Astronomy, The University of Arizona, Tucson, AZ 85721, USA*

ABSTRACT

With the distance sum rule in the Friedmann-Lemaître-Robertson-Walker metric, model-independent constraints on both the Hubble constant H_0 and spatial curvature Ω_K can be obtained using strong lensing time-delay data and Type Ia supernova (SN Ia) luminosity distances. This method is limited by the relative low redshifts of SNe Ia, however. Here, we propose using quasars as distance indicators, extending the coverage to encompass the redshift range of strong lensing systems. We provide a novel and improved method of determining H_0 and Ω_K simultaneously. By applying this technique to the time-delay measurements of seven strong lensing systems and the known ultraviolet versus X-ray luminosity correlation of quasars, we constrain the possible values of both H_0 and Ω_K , and find that $H_0 = 75.3^{+3.0}_{-2.9}$ km s⁻¹ Mpc⁻¹ and $\Omega_K = -0.01^{+0.18}_{-0.17}$. The measured Ω_K is consistent with zero spatial curvature, indicating that there is no significant deviation from a flat universe. If we use flatness as a prior, we infer that $H_0 = 75.3^{+1.9}_{-1.9}$ km s⁻¹ Mpc⁻¹, representing a precision of 2.5%. If we further combine these data with the 1048 current Pantheon SNe Ia, our model-independent constraints can be further improved to $H_0 = 75.3^{+3.0}_{-2.9}$ km s⁻¹ Mpc⁻¹ and $\Omega_K = 0.05^{+0.16}_{-0.14}$. In every case, we find that the Hubble constant measured with this technique is strongly consistent with the value (~ 74 km s⁻¹ Mpc⁻¹) measured using the local distance ladder, as opposed to the value optimized by *Planck*.

Keywords: cosmology: observations — cosmological parameters — distance scale — gravitational lensing: strong — quasars: general

1. INTRODUCTION

The Hubble constant H_0 characterizes the current expansion rate of the Universe and determines its absolute distance scale. In recent years, the accuracy of measuring H_0 has been significantly improved, but the value of H_0 ($= 67.4 \pm 0.5$ km s⁻¹ Mpc⁻¹; [Planck Collaboration et al. 2018](#)) inferred from *Planck* observations of the cosmic microwave background (CMB) in the context of flat Λ CDM represents a 4.4σ tension with that measured from local type Ia supernovae (SNe Ia) calibrated by the Cepheid distance ladder ($H_0 = 74.03 \pm 1.42$ km s⁻¹ Mpc⁻¹; [Riess et al. 2019](#)). Other early-Universe probes, such as a combination of clustering and weak lensing, baryon acoustic oscillations, and big-bang nucleosynthesis, yield results similar to the CMB ([Abbott et al. 2018](#)), while an alternate local calibration of the distance ladder using the tip of the red giant branch finds an intermediate value of H_0 ([Freedman et al. 2019, 2020](#); but see [Yuan et al. 2019](#)).

A review for the current status of the Hubble tension may be found in [Verde et al. \(2019\)](#). If the systematic errors of the observations cannot account for the discrepancy, this Hubble tension may indicate new physics beyond the standard Λ CDM cosmological model.

To better understand the origin of the tension, more independent determinations of H_0 are required. Strong gravitational lensing provides an independent method of measuring H_0 ([Refsdal 1964](#)). The time delay between strongly lensed images of variable sources is related to a quantity called the “time-delay distance”, $D_{\Delta t}$, which depends on the lensing potential. The quantity $D_{\Delta t}$ is a ratio of three angular diameter distances between the observer, lens, and source, and is primarily sensitive to H_0 , but also weakly dependent on other cosmological parameters. Thus, the Hubble constant H_0 can be constrained by these sources. This method is completely independent of, and complementary to, both the CMB and distance ladder analyses. Measuring H_0 in this manner, however, one has to assume a background cosmology. Recently, the H_0 Lenses in COSMOGRAIL’s Wellspring (H0LiCOW) collaboration derived $H_0 = 73.3^{+1.7}_{-1.8}$ km s⁻¹ Mpc⁻¹ for flat

Λ CDM using a sample of six gravitational lens time delays. The value of H_0 changed to $81.6^{+4.9}_{-5.3}$ km s⁻¹ Mpc⁻¹, however, for flat w CDM, in which the dark-energy equation of state is not fixed to -1 a priori (Wong et al. 2019). Obviously, the inferred value of H_0 using time-delay cosmography is strongly model dependent.

Instead of computing the time-delay distances within a specific cosmological model, one can determine the angular diameter distances from the observer to the source and lens through observations of SNe Ia to obtain model-independent constraints on H_0 (e.g., Aubourg et al. 2015; Cuesta et al. 2015; Collett et al. 2019; Liao et al. 2019, 2020; Pandey et al. 2019). But the relation of these two distances and the angular diameter distance from the lens to the source can not be determined directly from the observations. These three distances in the Friedmann-Lemaître-Robertson-Walker (FLRW) metric are connected via the distance sum rule, which depends on the curvature parameter of the Universe. In turn, under the assumption that the Universe is described by the FLRW metric, both H_0 and the spatial curvature can be estimated independently of the model by combining observations of strong lensing and SNe Ia (Collett et al. 2019). Furthermore, the comparison of the inferred values of the cosmic curvature from two or more lens-source pairs provides a consistency test of the FLRW metric (Räsänen et al. 2015). Based on the sum rule of distances along null geodesics of the FLRW metric, model-independent determinations of the spatial curvature have been implemented by combining strong gravitational lensing systems with other distance indicators, including SNe Ia (Räsänen et al. 2015; Liao et al. 2017, 2019, 2020; Xia et al. 2017; Denissenya et al. 2018; Li et al. 2018a; Collett et al. 2019; Zhou & Li 2020), gravitational waves (GWs; Liao 2019), and compact radio sources (Qi et al. 2019b). Such model-independent curvature determinations have also been proposed using future time delay measurements of strongly lensed transients (such as fast radio bursts, GWs, and SNe) and luminosity distances of SNe Ia (Li et al. 2018b, 2019; Qi et al. 2019a).

Among these studies, Collett et al. (2019) was the first to apply such a method to real data. They used combined observations of strong lensing time delays and SN Ia luminosity distances to determine not only the spatial curvature but also H_0 without adopting any particular model (see also Liao et al. 2019, 2020). It must be emphasized, however, that SNe Ia may be seen only up to $z \sim 2$, while the redshifts of the lens sources detected by the Large Synoptic Survey Telescope (LSST) would reach $z \sim 5$ (Liao et al. 2017). We can therefore only employ a small fraction of the lensing data that overlaps with the observed SNe Ia for this analysis. Using the distance sum rule would benefit considerably from the use of other distance indicators extending to higher redshifts, thus

taking full advantage of the whole lensing catalog. Thanks to their high luminosities, quasars have been viewed as promising cosmological probes. One can estimate their luminosity distances based on a nonlinear correlation between their ultraviolet (UV) and X-ray monochromatic luminosities. Although this correlation has been known for more than 30 years (Avni & Tananbaum 1986), only recently has the uncomfortably large dispersion in the relation been mitigated by refining the selection technique and flux measurements (Risaliti & Lusso 2015, 2019; Lusso & Risaliti 2016, 2017). This offers the possibility of using quasars as distance indicators, extending to redshifts ~ 6 . In this paper, we propose to use the wide redshift coverage of quasars to fully exploit sample of strong lensing systems in the LSST, in order to simultaneously measure H_0 and the spatial curvature, with the hope of providing more stringent constraints. In this paper, we use the updated H0LiCOW and STRong-lensing Insights into Dark Energy Survey (STRIDES) dataset consisting of seven lenses (Wong et al. 2019; Shajib et al. 2020) in order to extract the time-delay distances, and use the recently compiled, high-quality catalogue of 1598 UV and X-ray flux measurements of quasars covering the redshift range $0.035 < z < 5.1$ (Risaliti & Lusso 2019) to obtain the distance-redshift relation.

The outline of this paper is as follows. In Section 2, we describe the methodology and observations used for our analysis. Model-independent constraints on H_0 and Ω_K are presented in Section 3. Finally, a brief summary and discussion are presented in Section 4.

2. METHODOLOGY AND DATA

In a homogeneous and isotropic space, the spacetime geometry of the Universe can be described by the FLRW metric

$$ds^2 = -c^2 dt^2 + a^2(t) \left(\frac{dr^2}{1-Kr^2} + r^2 d\Omega^2 \right), \quad (1)$$

where $a(t) = 1/(1+z)$ is the scale factor and the constant K determines the spatial curvature. The present value of the Hubble parameter $H(z) \equiv \dot{a}/a$ is labeled H_0 . Let $D_A(z_l, z_s)$ denote the angular diameter distance of a source at redshift z_s (corresponding to emission time t_s) as observed at redshift z_l . Assuming that geometrical optics holds, the dimensionless comoving distance $d(z_l, z_s) \equiv (1+z_s)H_0 D_A(z_l, z_s)/c$ (which is independent of H_0) is then given by

$$d(z_l, z_s) = \frac{1}{\sqrt{|\Omega_K|}} \text{sinn} \left(\sqrt{|\Omega_K|} \int_{z_l}^{z_s} \frac{H_0}{H(z)} dz \right), \quad (2)$$

where $\Omega_K \equiv -K/H_0^2$ is the curvature parameter. Also, sinn is \sinh when $\Omega_K > 0$ and \sin when $\Omega_K < 0$. For a flat Universe with $\Omega_K = 0$, Equation (2) simplifies to a linear function of the integral. For convenience, we define $d(z) \equiv d(0, z)$,

Table 1. Redshifts and time-delay distances for the six H0LiCOW lenses and one STRIDES lens

Lens name	z_l	z_s	$D_{\Delta t}$ (Mpc)	References
B1608+656	0.6304	1.394	5156^{+296}_{-236}	Suyu et al. (2010); Jee et al. (2019)
RXJ1131-1231	0.295	0.654	2096^{+98}_{-83}	Suyu et al. (2014); Chen et al. (2019)
HE 0435-1223	0.4546	1.693	2707^{+183}_{-168}	Wong et al. (2017); Chen et al. (2019)
SDSS 1206+4332	0.745	1.789	5769^{+589}_{-471}	Birrer et al. (2019)
WFI2033-4723	0.6575	1.662	4784^{+399}_{-248}	Rusu et al. (2019)
PG 1115+080	0.311	1.722	1470^{+130}_{-127}	Chen et al. (2019)
DES J0408-5354	0.597	2.375	3382^{+146}_{-115}	Lin et al. (2017); Shajib et al. (2020)

$d_l \equiv d(0, z_l)$, $d_s \equiv d(0, z_s)$, and $d_{ls} \equiv d(z_l, z_s)$. If $d(z)$ is monotonic and $d'(z) > 0$, then these dimensionless distances in the FLRW frame are related via the distance sum rule (Peebles 1993; Bernstein 2006; Räsänen et al. 2015):

$$d_{ls} = d_s \sqrt{1 + \Omega_K d_l^2} - d_l \sqrt{1 + \Omega_K d_s^2}. \quad (3)$$

It is worth noting that the FLRW metric can be ruled out if the derived Ω_K from the combination of distances (d_l , d_s , and d_{ls}) are observationally found to be unequal for any two pairs of (z_l , z_s). Furthermore, Equation (3) can be rewritten as (Liao et al. 2017)

$$\frac{d_{ls}}{d_l d_s} = T(z_l) - T(z_s), \quad (4)$$

where

$$T(z) = \sqrt{1/d(z)^2 + \Omega_K}, \quad (5)$$

such that the distance $d(z)$ and the time-delay distance ratio $d_l d_s / d_{ls}$ (see below) are encoded.

In strong lensing, the measured time delay between two images of the source is related to both the geometry of the Universe and the gravitational potential of the lens galaxy via the relation

$$\Delta t = \frac{D_{\Delta t}}{c} \Delta \phi, \quad (6)$$

where $D_{\Delta t}$ is the time-delay distance and $\Delta \phi$ is the difference between the Fermat potentials of the two images. The time-delay distance is the combination of three angular angular diameter distances (Refsdal 1964; Schneider et al. 1992; Suyu et al. 2010):

$$D_{\Delta t} = (1 + z_l) \frac{D_l D_s}{D_{ls}} = \frac{c}{H_0} \frac{d_l d_s}{d_{ls}}, \quad (7)$$

where subscripts “l” and “s” stand for lens and source, respectively. $D_{\Delta t}$ has units of distance and is inversely proportional to H_0 . Therefore, with measurements of Δt , d_l , and d_s and an accurate lens model to estimate $\Delta \phi$, we can directly determine H_0 and Ω_K from Equations (4) and (7) without involving any specific cosmological model.

In this work, the time-delay distance ratio $d_l d_s / d_{ls}$ is extracted from strong gravitational lensing, while the other two distances (d_l and d_s) are obtained using the UV versus X-ray luminosity correlation in quasars.

2.1. Strong lensing data: time-delay distance ratios

Recently, the H0LiCOW collaboration presented the latest measurements of H_0 from a combined sample of six strong lensing systems with measured time delays (Wong et al. 2019). The six lenses are B1608+656 (Suyu et al. 2010; Jee et al. 2019), RXJ1131-1231 (Suyu et al. 2013, 2014; Chen et al. 2019), HE 0435-1223 (Wong et al. 2017; Chen et al. 2019), SDSS 1206+4332 (Birrer et al. 2019), WFI2033-4723 (Rusu et al. 2019), and PG 1115+080 (Chen et al. 2019). All lenses except B1608+656 were analyzed blindly with respect to the cosmological parameters. We summarize the lens and source redshifts (i.e., z_l and z_s), as well as the time-delay distance constraint $D_{\Delta t}$, for each individual lens in Table 1. The posterior distributions of the time-delay distances for the six lenses are available on the H0LiCOW website.¹ For the lens B1608+656, the time-delay distance likelihood function was given as a skewed log-normal distribution:

$$\mathcal{L}_{D_{\Delta t}} = \frac{1}{\sqrt{2\pi}(x - \lambda_D)\sigma_D} \exp\left[-\frac{(\ln(x - \lambda_D) - \mu_D)^2}{2\sigma_D^2}\right], \quad (8)$$

with the parameters $\mu_D = 7.0531$, $\sigma_D = 0.22824$, and $\lambda_D = 4000.0$, where $x = D_{\Delta t}/(1 \text{ Mpc})$. For the other five lenses, the posterior distributions of $D_{\Delta t}$ were released in the form of Monte Carlo Markov chains (MCMC). A kernel density estimator was used to compute $\mathcal{L}_{D_{\Delta t}}$ from the chains (Wong et al. 2019). Very recently, the STRIDES collaboration presented the most precise measurement of H_0 to date from a single time-delay lens DES J0408-5354 (Shajib et al. 2020). Table 1 also lists the redshifts and the measured time-delay distance for this lens. We use the time-delay distance posterior of DES J0408-5354 that was derived in Shajib et al. (2020).

Following Collett et al. (2019), we also use constraints from the double-source-plane strong lens SDSSJ0946+1006 (Gavazzi et al. 2008). The lensing galaxy in this system has a redshift of $z_l = 0.222$ and the redshift of the first source s_1 is $z_{s_1} = 0.609$ (Gavazzi et al. 2008), while the redshift of the second source s_2 is taken to be at the peak of the photo-

¹ <http://www.h0licow.org>

metric redshift probability from Collett & Auger (2014), i.e., $z_{s2} = 2.3$. The presence of two sources lensed by the same foreground galaxy offers an accurate constraint on the cosmological scaling factor

$$\beta \equiv \frac{d_{ls1}d_{s2}}{d_{s1}d_{ls2}} = \frac{d_{ls1}}{d_l d_{s1}} \cdot \frac{d_l d_{s2}}{d_{ls2}}. \quad (9)$$

Note that this ratio is sensitive to the curvature parameter Ω_K , being independent of H_0 . In SDSSJ0946+1006, the cosmological scaling factor is constrained to be $\beta^{-1} = 1.404 \pm 0.016$ (Collett & Auger 2014). That is, the posterior distribution of β^{-1} is well approximated by a Gaussian function centred at 1.404 with width $\sigma_{\beta^{-1}} = 0.016$. The likelihood function for β^{-1} is then given by

$$\mathcal{L}_{\beta^{-1}} = \frac{1}{\sqrt{2\pi}\sigma_{\beta^{-1}}} \exp \left\{ -\frac{\left[\beta^{-1} - \frac{T(z_l) - T(z_{s2})}{T(z_l) - T(z_{s1})} \right]^2}{2\sigma_{\beta^{-1}}^2} \right\}. \quad (10)$$

2.2. Quasar data: the distances d_l and d_s

In order to obtain model-independent measurements of H_0 and Ω_K via Equation (4), we also need to know the distance $d(z)$, which we here measure using the non-linear correlation between the UV and X-ray luminosities of quasars. After refining their selection technique and flux measurements, Risaliti & Lusso (2019) collected a final sample of 1598 quasars with reliable measurements of the intrinsic UV and X-ray emissions. We use this high-quality quasar catalog covering the redshift range $0.036 < z < 5.1$ for the analysis demonstrated in this paper. The non-linear luminosity relation of quasars, $\log_{10} L_X = \gamma \log_{10} L_{UV} + \kappa$, can be re-expressed in terms of the measured UV and X-ray fluxes, F_{UV} and F_X , and the luminosity distance, D_L , at redshift z , according to the expression

$$\log_{10} F_X = \kappa' + \gamma \log_{10} F_{UV} + 2(\gamma - 1) \log_{10} D_L, \quad (11)$$

where κ' is a parameter that subsumes the slope γ and intercept κ , i.e., $\kappa' = \kappa + (\gamma - 1) \log_{10} 4\pi$. The luminosity distance D_L can then be extracted from the fluxes as a function of γ and κ' . In practice, the parameter γ can be derived in a cosmology-independent way by directly fitting the relation between F_X and F_{UV} with sub-samples in narrow redshift intervals. Using this approach, one can verify the lack of evolution in this relation with redshift—an essential requirement for its implementation to obtain quasar distances. Risaliti & Lusso (2019) showed that the parameter γ does not display any significant evolution; it appears to be a constant at all redshifts. Its average value is $\gamma = 0.633 \pm 0.002$. The redshift dependence of the scaling parameter κ is difficult to test without a solid physical explanation for the $L_X - L_{UV}$ relation (Risaliti & Lusso 2015, 2019). Since its intrinsic value is still unknown, we may instead regard κ'

as an arbitrary scaling factor. But following the treatment of Risaliti & Lusso (2015, 2019), we adopt their average value of $\gamma (= 0.633 \pm 0.002)$ to estimate a scaling parameter-dependent D_L for each quasar using Equation (11).

With the distance-duality relation that holds true in any spacetime for any gravity theory (Etherington 1933; Ellis 2009), one can use the scaling parameter-dependent luminosity distance of quasars to obtain the dimensionless comoving angular diameter distances $d = H_0 D_L / c(1+z)$. In principle, we need to select those quasars whose redshift matches that of the lens and source in each system. It is difficult for this to be fulfilled for all discrete observed events, however. There are always differences between the lensing redshifts and the nearest quasars. This issue can be overcome by reconstructing a continuous distance function that best approximates the discrete observed data using a polynomial fit (Räsänen et al. 2015; Liao et al. 2017; Li et al. 2018a; Collett et al. 2019; Liao 2019; Zhou & Li 2020). In our analysis, we construct the dimensionless distance function $d(z)$ in a cosmology-independent way by fitting a third-order polynomial with initial conditions $d(0) = 0$ and $d'(0) = 1$, to the quasar data. This polynomial is expressed as

$$d(z) = z + a_1 z^2 + a_2 z^3, \quad (12)$$

where a_1 and a_2 are two free parameters that must be optimized along with the scaling parameter κ' and the intrinsic dispersion σ_{int} (see below). We find that a third-order polynomial is flexible enough to fit the current data, while higher order polynomials do not improve the goodness of fit, especially when taking into account the larger number of free parameters.

The high-redshift quasar sample contains a significant intrinsic dispersion σ_{int} , which has to be treated as an additional free parameter (Risaliti & Lusso 2015, 2019). Thus, the variance on each quasar is given by the quadratic sum of the measurement error of that quasar (σ_i) and σ_{int} . This leads to the following formula of the likelihood function:

$$\mathcal{L}_{\text{quasars}} = \prod_{i=1}^{1598} \frac{1}{\sqrt{2\pi(\sigma_i^2 + \sigma_{\text{int}}^2)}} \exp \left[-\frac{\Delta_i^2}{2(\sigma_i^2 + \sigma_{\text{int}}^2)} \right], \quad (13)$$

where

$$\Delta_i = \log_{10}(F_X)_i - \gamma \log_{10}(F_{UV})_i - \kappa' - 2(\gamma - 1) \log_{10} \left[\frac{c}{H_0} (1 + z_i) d(z_i) \right]. \quad (14)$$

In this likelihood estimation, there is a degeneracy between the Hubble constant H_0 and κ' . We therefore adopt a fiducial $H_0 = 70 \text{ km s}^{-1} \text{ Mpc}^{-1}$ for the sake of optimizing κ' . Another choice of H_0 would require a corresponding re-scaling of this optimized κ' .

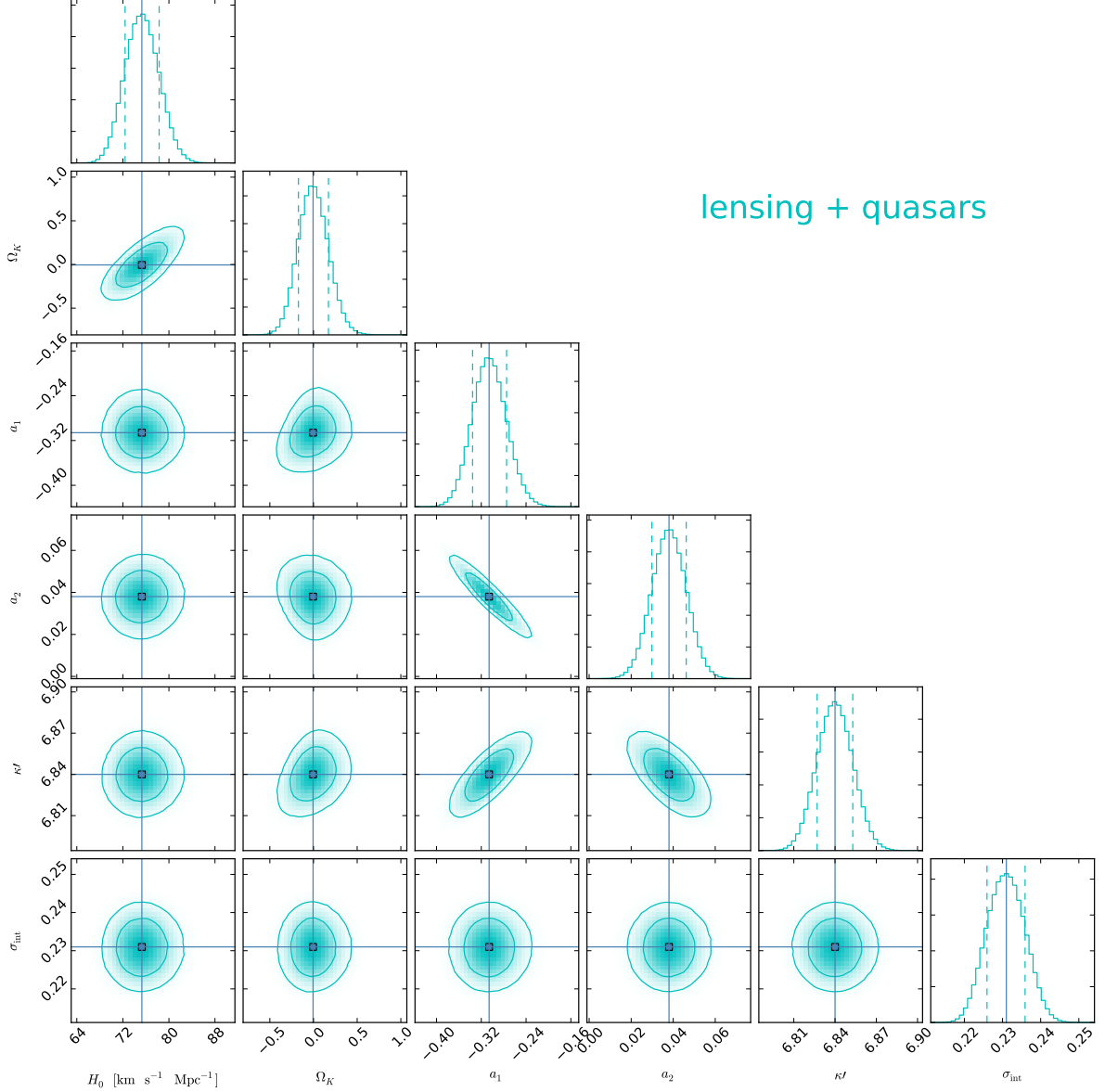


Figure 1. 1D and 2D marginalized probability distributions with 1σ and 2σ confidence contours for the parameters H_0 , Ω_K , a_1 , a_2 , κ' , and σ_{int} constrained by the strong lensing systems and quasars. The vertical solid lines represent the medium values, and the vertical dashed lines enclose the 68% credible region.

3. MODEL-INDEPENDENT CONSTRAINTS ON H_0 AND Ω_K

The quantities $d(z)$, H_0 , and Ω_K are fitted to the strong lensing and quasar data simultaneously using the Python MCMC module EMCEE (Foreman-Mackey et al. 2013). The final log-likelihood sampled by EMCEE is a sum of the separate likelihoods of the time delay lenses, double-source-plane strong lens, and high-redshift quasars:

$$\ln(\mathcal{L}_{\text{tot}}) = \ln(\mathcal{L}_{D_{\Delta t}}) + \ln(\mathcal{L}_{\beta^{-1}}) + \ln(\mathcal{L}_{\text{quasars}}). \quad (15)$$

The third-order polynomial has two free parameters (a_1 and a_2). The scaling parameter κ' and the intrinsic dispersion σ_{int}

enter into the quasar likelihood as two nuisance parameters. In addition, $d_l d_s / d_{ls}$ given by Equation (4) involves the curvature parameter Ω_K and the time-delay distance given by Equation (7) depends on H_0 , making it six free parameters in total.

The 1D marginalized probability distributions and 2D regions with 1σ and 2σ contours corresponding to these six parameters, constrained by the lensing + quasar data, are displayed in Figure 1. These contours show that, at the 68% confidence level, the median values and the 16th and 84th percentiles are $H_0 = 75.3^{+3.0}_{-2.9} \text{ km s}^{-1} \text{ Mpc}^{-1}$, $\Omega_K = -0.01^{+0.18}_{-0.17}$, $a_1 = -0.306^{+0.031}_{-0.030}$, $a_2 = 0.038^{+0.008}_{-0.008}$, $\kappa' = 6.840^{+0.013}_{-0.013}$, and $\sigma_{\text{int}} =$

Table 2. Constraints on All Parameters with Various Choices of Data

Data	H_0 ($\text{km s}^{-1} \text{Mpc}^{-1}$)	Ω_K	a_1	a_2	κ'	σ_{int}	M_B
lensing+quasars	$75.3^{+3.0}_{-2.9}$	$-0.01^{+0.18}_{-0.17}$	$-0.306^{+0.031}_{-0.030}$	$0.038^{+0.008}_{-0.008}$	$6.840^{+0.013}_{-0.013}$	$0.231^{+0.005}_{-0.005}$	—
lensing+quasars	$75.3^{+1.9}_{-1.9}$	0 (fixed)	$-0.301^{+0.029}_{-0.028}$	$0.037^{+0.008}_{-0.008}$	$6.841^{+0.012}_{-0.012}$	$0.231^{+0.005}_{-0.005}$	—
lensing+SNe Ia	$75.9^{+3.1}_{-3.1}$	$0.16^{+0.22}_{-0.20}$	$-0.259^{+0.017}_{-0.017}$	$0.032^{+0.012}_{-0.012}$	—	—	$-19.344^{+0.011}_{-0.011}$
lensing+SNe Ia	$74.3^{+1.9}_{-1.9}$	0 (fixed)	$-0.252^{+0.015}_{-0.015}$	$0.025^{+0.008}_{-0.008}$	—	—	$-19.346^{+0.010}_{-0.010}$
lensing+quasars+SNe Ia	$75.3^{+3.0}_{-2.9}$	$0.05^{+0.16}_{-0.14}$	$-0.260^{+0.012}_{-0.012}$	$0.027^{+0.004}_{-0.004}$	$6.856^{+0.008}_{-0.008}$	$0.231^{+0.005}_{-0.005}$	$-19.341^{+0.009}_{-0.009}$
lensing+quasars+SNe Ia	$74.5^{+1.7}_{-1.7}$	0 (fixed)	$-0.259^{+0.012}_{-0.012}$	$0.026^{+0.004}_{-0.004}$	$6.856^{+0.008}_{-0.008}$	$0.231^{+0.005}_{-0.005}$	$-19.341^{+0.009}_{-0.009}$

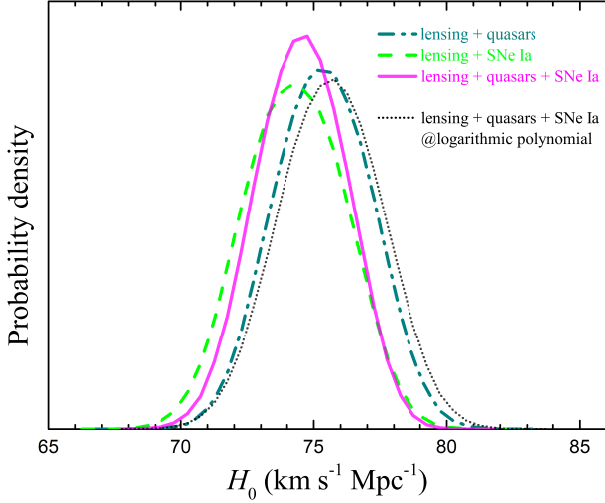


Figure 2. 1D marginalized probability distributions of the Hubble constant H_0 in a flat Universe constrained from the lensing + quasar data (dot-dashed curve), the lensing + SN Ia data (dashed curve), and the combined lensing + quasar + SN Ia data (solid curve), respectively, using a linear polynomial function. The dotted curve corresponds to the analysis of the lensing + quasar + SN Ia data using a logarithmic polynomial function.

$0.231^{+0.005}_{-0.005}$. If we instead assume zero spatial curvature, the marginalized probability distribution for H_0 is shown in Figure 2 (dot-dashed curve). This model-independent constraint yields $H_0 = 75.3^{+1.9}_{-1.9} \text{ km s}^{-1} \text{Mpc}^{-1}$. The corresponding results for the lensing + quasar data are summarized in lines 1 and 2 of Table 2 for a non-flat and flat Universe. The comparison between these two cases indicates that the nuisance parameters (a_1 , a_2 , κ' , and σ_{int}) have little effect on the cosmological parameters.

For this analysis, we have used the average value (0.633) of the slope γ in the quasar luminosity relation (Eqn. 11), estimated within narrow redshift bins, as described in Section 2.2. Melia (2019) tested the dependence of this slope on the choice of cosmological model, and found that it appears to be very weakly dependent on the expansion rate as well, showing that γ falls within the relatively narrow range of (0.626, 0.640) for three diverse formulations of the luminosity distance D_L . To investigate how sensitive our results

on H_0 and Ω_K are on the choice of γ within this range, we also perform two parallel comparative analyses of the lensing + quasar data using $\gamma = 0.626$ and 0.640 . For the latter, we find $H_0 = 75.5^{+3.0}_{-2.9} \text{ km s}^{-1} \text{Mpc}^{-1}$ and $\Omega_K = 0.04^{+0.17}_{-0.16}$. For the former, we get $H_0 = 75.1^{+3.0}_{-2.9} \text{ km s}^{-1} \text{Mpc}^{-1}$ and $\Omega_K = -0.05^{+0.18}_{-0.17}$. The values of H_0 and Ω_K change only slightly as γ is varied, with the largest variation lying within $\approx 0.2\sigma$ of the optimized values, well within the uncertainty. So there is no concern regarding a possibly large dependence on γ . For the rest of the paper, we shall therefore adopt the average value $\gamma = 0.633$ estimated by Risaliti & Lusso (2019) in their study of narrow redshift bins.

The SNe Ia are often adopted as distance indicators for providing the distance $d(z)$ on the right side of Equation (4) (see, e.g., Räsänen et al. 2015; Li et al. 2018a; Liao et al. 2019, 2020; Collett et al. 2019). To compare our results with previous work, we therefore also carry out our model-independent analysis using a combination of data that includes the latest Pantheon SN Ia observations, and see if one can further constrain the comoving distance $d(z)$. Scolnic et al. (2018) recently released the largest combined sample of SNe Ia referred to as Pantheon, consisting of 1048 SNe Ia in the redshift range of $0.01 < z < 2.3$. The distance modulus of a Type Ia SN can be determined using the Spectral Adaptive Light curve Template 2 (SALT2) light-curve fit parameters, based on the formula $\mu = m_B - M_B + \alpha X_1 - \eta C + \Delta_M + \Delta_B$, where m_B is the observed B -band apparent magnitude, X_1 is the light-curve stretch factor, C is the color, Δ_M is a distance correction based on the host galaxy mass, and Δ_B denotes a distance correction based on predicted biases from simulations. Furthermore, α and η are nuisance coefficients of the luminosity-stretch and luminosity-color relations, respectively, and M_B is another nuisance parameter that describes the absolute B -band magnitude of a fiducial SN.

In general, the two nuisance parameters α and η should be optimized simultaneously with the cosmological parameters for each specific cosmological model. In this case, the derived SN distances are model-dependent. To dodge this problem, Kessler & Scolnic (2017) introduced the BEAMS with Bias Corrections (BBC) method to correct those expected biases and simultaneously fit for the α and η parameters. This method relies on the approach proposed by Marriner et al.

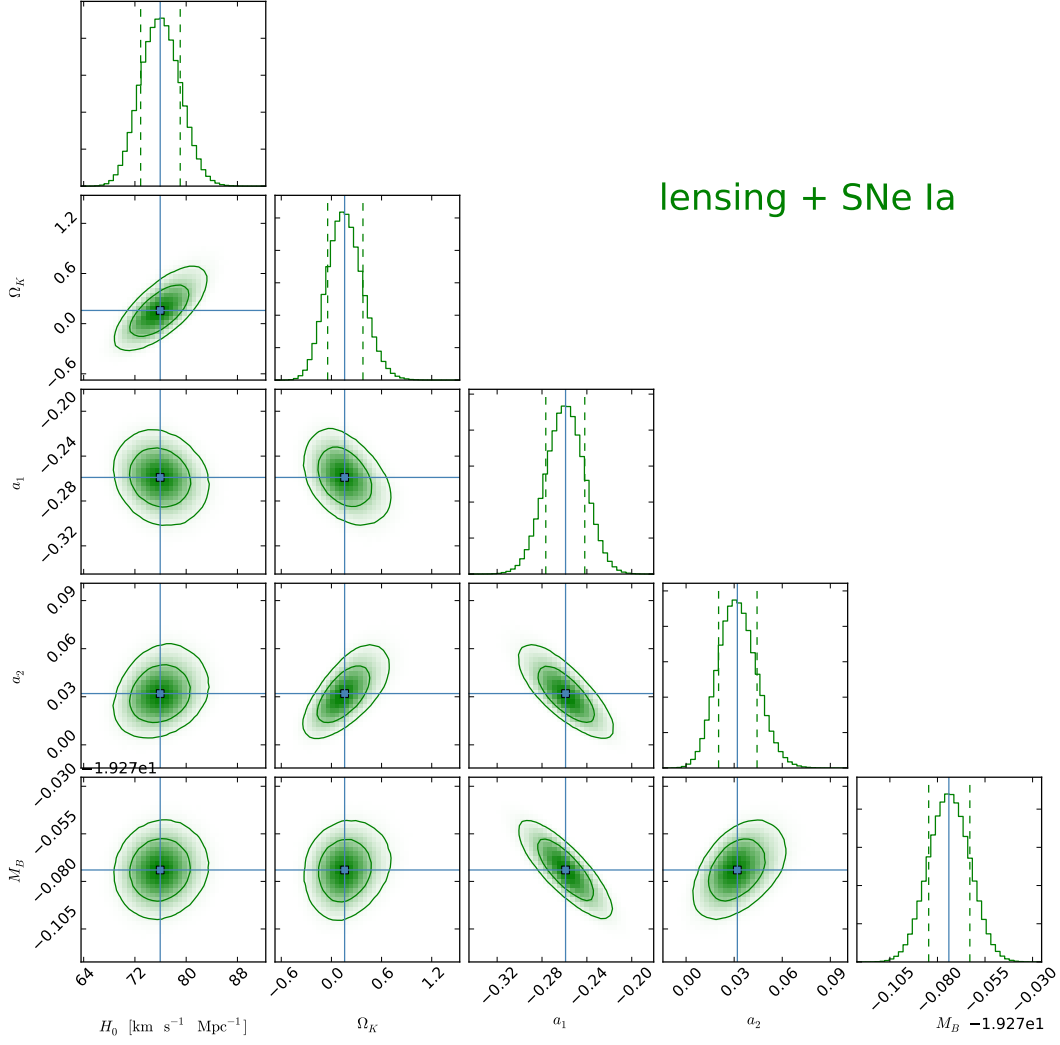


Figure 3. Same as Figure 1, but now showing the constraints for the parameters H_0 , Ω_K , a_1 , a_2 , and M_B based on the analysis of the combined strong lensing and Pantheon SN Ia data only.

(2011), but involves extensive simulations for correcting the SALT2 light-curve fitter. The BBC fit creates a bin-averaged Hubble diagram of SNe Ia, and then the coefficients α and η are inferred by fitting to a reference cosmological model. The reference cosmology is supposed to reproduce the local shape of the Hubble diagram within each redshift bin. If there are sufficient redshift bins, the fitted coefficients α and η will converge to consistent values, which are independent of the reference cosmology (Marriner et al. 2011). With the BBC method, Scolnic et al. (2018) reported the corrected apparent magnitudes $m_{\text{corr}} = \mu + M_B$ for all the Pantheon SNe. Therefore, we just need to subtract M_B from m_{corr} to obtain the observed distance modulus μ . For the SN data set, the uncertainties are given by a covariance matrix \mathbf{C} (including both statistical and systematic uncertainties). Given a vector of distance residuals of the SN sample that may be defined as $\Delta\hat{\mu} = \hat{\mu} - \hat{\mu}_{\text{model}}$, where $\hat{\mu}$ ($\hat{\mu}_{\text{model}}$) is the observed (model)

vector of distance moduli, the likelihood of the model fit is expressed as

$$-2\ln(\mathcal{L}_{\text{SN}}) = \Delta\hat{\mu}^T \cdot \mathbf{C}^{-1} \cdot \Delta\hat{\mu}. \quad (16)$$

Here the model vector $\hat{\mu}_{\text{model}}$ is determined by $\mu_{\text{model},i} = 5\log_{10}[D_L(\mathcal{P}, z_i)/10 \text{ pc}] = 5\log_{10}[(1+z_i)d(\mathcal{P}, z_i)] + M_{H_0}$, where $M_{H_0} = -5\log_{10}(10 \text{ pc } H_0/c)$ and \mathcal{P} denotes the model parameters. Given the degeneracy with the absolute magnitude M_B , the value of M_{H_0} is arbitrary and we fix it to $M_{H_0} = 43.16$ (corresponding to the aforementioned fiducial $H_0 = 70 \text{ km s}^{-1} \text{ Mpc}^{-1}$).

We first analyze the lensing + Pantheon SN Ia data. In this case, the log-likelihood sampled by EMCEE becomes

$$\ln(\mathcal{L}_{\text{tot}}) = \ln(\mathcal{L}_{D_{\Delta t}}) + \ln(\mathcal{L}_{\beta^{-1}}) + \ln(\mathcal{L}_{\text{SN}}). \quad (17)$$

There are five free parameters, including the Hubble constant H_0 , the curvature parameter Ω_K , the two polynomial

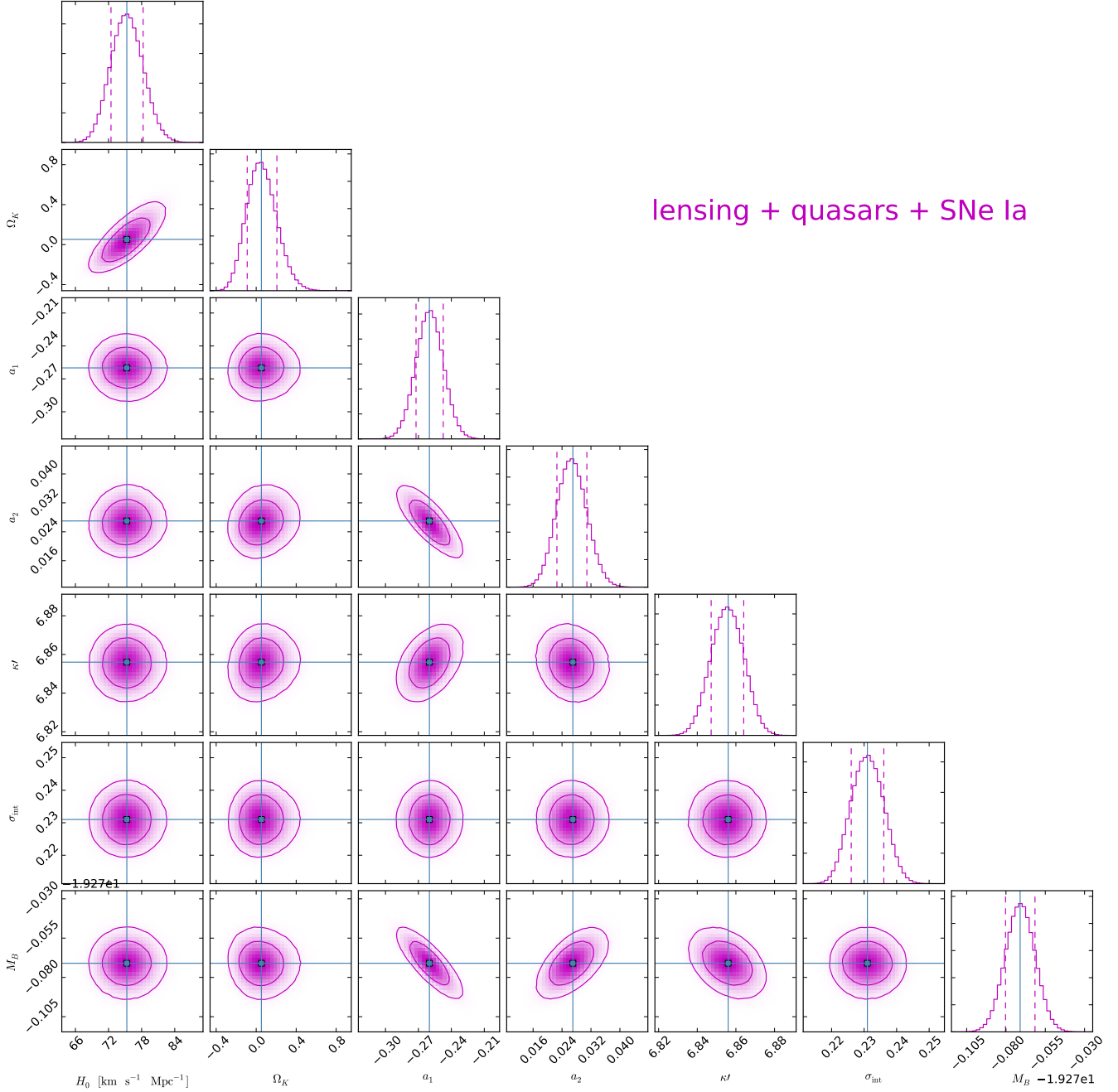


Figure 4. Same as Figure 1, but now showing the constraints for the parameters H_0 , Ω_K , a_1 , a_2 , κ' , σ_{int} , and M_B based on the analysis of the combined strong lensing, quasar, and Pantheon SN Ia data.

coefficients (a_1 and a_2), and the SN absolute magnitude M_B . These parameters are constrained to be $H_0 = 75.9^{+3.1}_{-3.1}$ km s⁻¹ Mpc⁻¹, $\Omega_K = 0.16^{+0.22}_{-0.20}$, $a_1 = -0.259^{+0.017}_{-0.017}$, $a_2 = 0.032^{+0.012}_{-0.012}$, and $M_B = -19.344^{+0.011}_{-0.011}$, which are presented in Figure 3 and Table 2. If a prior of flatness (i.e., $\Omega_K = 0$) is adopted, the marginalized H_0 constraint is $H_0 = 74.3^{+1.9}_{-1.9}$ km s⁻¹ Mpc⁻¹ (see dashed curve in Figure 2). The comparison between lines 1 and 3 of Table 2 suggests that the constraint precisions of H_0

and Ω_K obtained using the lensing + quasar data are slightly better than those from the lensing + SN Ia data.

We also carry out this type of analysis using the combined strong lensing + quasar + Pantheon SN Ia data sets. The final log-likelihood sampled by EMCEE now becomes

$$\ln(\mathcal{L}_{\text{tot}}) = \ln(\mathcal{L}_{D_{\Delta t}}) + \ln(\mathcal{L}_{\beta^{-1}}) + \ln(\mathcal{L}_{\text{quasars}}) + \ln(\mathcal{L}_{\text{SN}}). \quad (18)$$

In this case, the free parameters are the Hubble constant H_0 , the curvature parameter Ω_K , the two polynomial coefficients

(a_1 and a_2), the parameters characterizing the quasar luminosity relation (κ' and σ_{int}), and the SN absolute magnitude M_B . As shown in Figure 4 and Table 2, the marginalized distributions give $H_0 = 75.3^{+3.0}_{-2.9}$ km s⁻¹ Mpc⁻¹, $\Omega_K = 0.05^{+0.16}_{-0.14}$, $a_1 = -0.260^{+0.012}_{-0.012}$, $a_2 = 0.027^{+0.004}_{-0.004}$, $\kappa' = 6.856^{+0.008}_{-0.008}$, $\sigma_{\text{int}} = 0.231^{+0.005}_{-0.005}$, and $M_B = -19.341^{+0.009}_{-0.009}$. We see that, compared to the results obtained using solely the strong lensing and quasar observations, somewhat more precise constraints may be achieved for H_0 and Ω_K by also including the SNe Ia data. The marginalized constraint on H_0 assuming a flat Universe is shown in Figure 2 (solid curve), and is given by $H_0 = 74.5^{+1.7}_{-1.7}$ km s⁻¹ Mpc⁻¹.

4. SUMMARY AND DISCUSSION

Based on the sum rule of distances along null geodesics of the FLRW metric, we can obtain model-independent constraints on both the Hubble constant H_0 and spatial curvature Ω_K by confronting observations of strong lensing time delays with SN Ia luminosity distances. In this paper, aiming to mitigate the redshift limitation of using solely SNe Ia as distance indicators, we have proposed using high- z quasars to provide the distances required by the sum rule. Combining the time delay measurements of six H0LiCOW lenses and one STRIDES lens with the known UV versus X-ray luminosity correlation of 1598 quasars, we have simultaneously placed limits on H_0 and Ω_K without assuming any specific cosmological model. This analysis suggests that the curvature parameter is constrained to be $\Omega_K = -0.01^{+0.18}_{-0.17}$, consistent with a flat Universe. Meanwhile, the optimized Hubble constant is $H_0 = 75.3^{+3.0}_{-2.9}$ km s⁻¹ Mpc⁻¹. If instead we assume a spatially flat universe, we find $H_0 = 75.3^{+1.9}_{-1.9}$ km s⁻¹ Mpc⁻¹, representing a precision of 2.5%, in good agreement with the measurement of H_0 using SNe Ia calibrated by the local distance ladder which, however, is in 4.0σ tension with the value inferred by *Planck* from CMB measurements. These model-independent results are fully consistent with the Hubble constant inferred previously from the H0LiCOW data assuming a flat Λ CDM model (Wong et al. 2019).

We also carried out this type of analysis using the combined strong lensing + Pantheon SN Ia data sets and the combined strong lensing + quasar + Pantheon SN Ia data sets, respectively. For the former, we found that the model-independent constraints are $H_0 = 75.9^{+3.1}_{-3.1}$ km s⁻¹ Mpc⁻¹ and $\Omega_K = 0.16^{+0.22}_{-0.20}$, which are slightly worse than the constraint precisions obtained with the lensing + quasar data. For the latter, we found that the constraints on H_0 and Ω_K may be improved somewhat, yielding $H_0 = 75.3^{+3.0}_{-2.9}$ km s⁻¹ Mpc⁻¹ and $\Omega_K = 0.05^{+0.16}_{-0.14}$. And if a flat Universe is assumed as a prior, one derives the optimized value $H_0 = 74.3^{+1.9}_{-1.9}$ km s⁻¹ Mpc⁻¹ (representing a 2.6% precision measurement) for the former case, and $H_0 = 74.5^{+1.7}_{-1.7}$ km s⁻¹ Mpc⁻¹ (representing a 2.3% precision measurement) for the latter case.

Previously, Wong et al. (2019) obtained $H_0 = 74.4^{+2.1}_{-2.3}$ km s⁻¹ Mpc⁻¹ and $\Omega_K = 0.26^{+0.17}_{-0.25}$ by analyzing six time-delay lenses in the non-flat Λ CDM model. Collett et al. (2019) used time delay lens and SNe Ia to obtain model-independent constraints of $H_0 = 75.7^{+4.5}_{-4.4}$ km s⁻¹ Mpc⁻¹ and $\Omega_K = 0.12^{+0.27}_{-0.25}$ by implementing a polynomial fitting to the supernova luminosity distances. And by using Gaussian processes to extract the supernova distances, Liao et al. (2020) obtained model-independent determinations of $H_0 = 77.3^{+2.2}_{-3.0}$ km s⁻¹ Mpc⁻¹ and $\Omega_K = 0.33^{+0.12}_{-0.19}$ from strong lensing and SN Ia data. Comparing our results to these previous constraints, it is quite apparent that our method is at least competitive with these other approaches. Most importantly, our method offers a new model-independent way of simultaneously constraining both H_0 and Ω_K .

Finally, we considered whether our choice of parametrization for the dimensionless distance $d(z)$ (as a linear polynomial function; see Equation 12) might be affecting the results. To test the dependence of the outcome on the functional form of $d(z)$, we also carried out a parallel comparative analysis of the lensing + quasar + SN Ia data using a logarithmic polynomial function, i.e., $d(z) = \ln(10)[\log_{10}(1+z) + a_1 \log_{10}^2(1+z) + a_2 \log_{10}^3(1+z)]$, like that used by Risaliti & Lusso (2019), and the results are summarized in Figure 5. Using the logarithmic polynomial fit, we found that the constraints are $H_0 = 76.3^{+3.0}_{-2.9}$ km s⁻¹ Mpc⁻¹, $\Omega_K = 0.05^{+0.16}_{-0.15}$, $a_1 = 0.736^{+0.084}_{-0.083}$, $a_2 = -1.218^{+0.224}_{-0.219}$, $\kappa' = 6.857^{+0.008}_{-0.009}$, $\sigma_{\text{int}} = 0.231^{+0.005}_{-0.005}$, and $M_B = -19.357^{+0.013}_{-0.013}$. Assuming a zero spatial curvature, we got $H_0 = 75.6^{+1.9}_{-1.9}$ km s⁻¹ Mpc⁻¹ (see dotted curve in Figure 2; representing a precision of 2.5%), $a_1 = 0.747^{+0.075}_{-0.075}$, $a_2 = -1.248^{+0.193}_{-0.189}$, $\kappa' = 6.857^{+0.008}_{-0.008}$, $\sigma_{\text{int}} = 0.231^{+0.005}_{-0.005}$, and $M_B = -19.358^{+0.013}_{-0.013}$. The differences between these optimized cosmological parameters and those obtained with the linear polynomial fit are well within the 1σ errors. Thus, the adoption of a different functional form for $d(z)$ has only a minimal influence on these results.

We would like to thank the anonymous referee for constructive comments which helped improve our work. We are also grateful to Anowar Jaman Shajib for sharing the distance posteriors of the lens DES J0408-5354, and to Shen-Shi Du for his kind help. This work is partially supported by the National Natural Science Foundation of China (grant Nos. 11673068, 11725314, and U1831122), the Youth Innovation Promotion Association (2017366), the Key Research Program of Frontier Sciences (grant Nos. QYZDB-S5W-SYS005 and ZDBS-LY-7014), the Strategic Priority Research Program “Multi-waveband gravitational wave universe” (grant No. XDB23000000) of Chinese Academy of Sciences, and the Guangxi Key Laboratory for Relativistic Astrophysics.

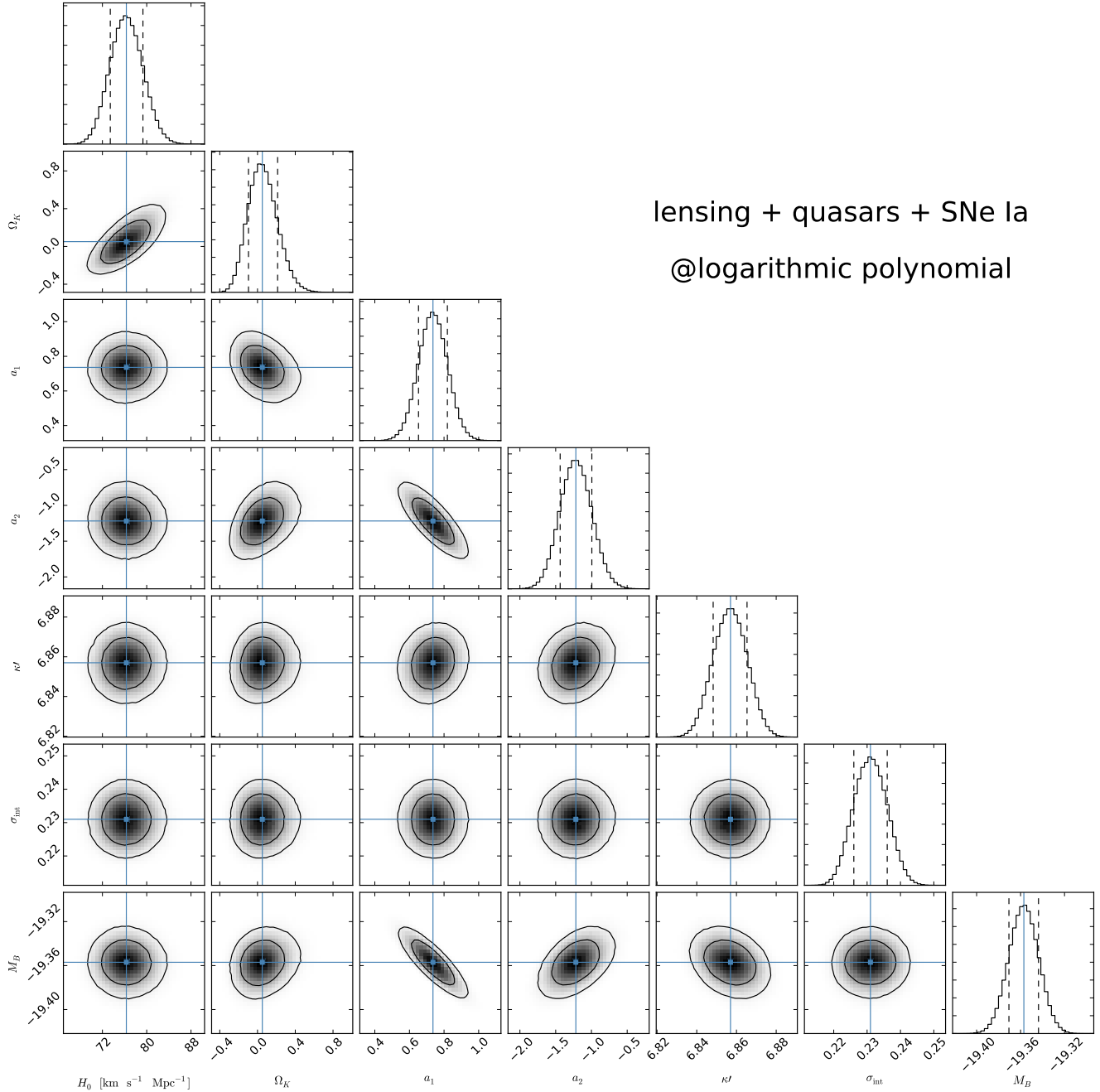


Figure 5. Same as Figure 4, but now showing the constraints based on the analysis of the combined lensing + quasar + SN Ia data using a logarithmic polynomial function.

REFERENCES

- Abbott, T. M. C., Abdalla, F. B., Annis, J., et al. 2018, *MNRAS*, 480, 3879
- Aubourg, É., Bailey, S., Bautista, J. E., et al. 2015, *PhRvD*, 92, 123516
- Avni, Y., & Tananbaum, H. 1986, *ApJ*, 305, 83
- Bernstein, G. 2006, *ApJ*, 637, 598
- Birrer, S., Treu, T., Rusu, C. E., et al. 2019, *MNRAS*, 484, 4726
- Chen, G. C. F., Fassnacht, C. D., Suyu, S. H., et al. 2019, *MNRAS*, 490, 1743
- Collett, T., Montanari, F., & Räsänen, S. 2019, *PhRvL*, 123, 231101
- Collett, T. E., & Auger, M. W. 2014, *MNRAS*, 443, 969
- Cuesta, A. J., Verde, L., Riess, A., & Jimenez, R. 2015, *MNRAS*, 448, 3463

- Denissenya, M., Linder, E. V., & Shafieloo, A. 2018, JCAP, 2018, 041
- Ellis, G. F. R. 2009, *General Relativity and Gravitation*, 41, 581
- Etherington, I. M. H. 1933, *Philosophical Magazine*, 15, 761
- Foreman-Mackey, D., Hogg, D. W., Lang, D., & Goodman, J. 2013, *PASP*, 125, 306
- Freedman, W. L., Madore, B. F., Hatt, D., et al. 2019, *ApJ*, 882, 34
- Freedman, W. L., Madore, B. F., Hoyt, T., et al. 2020, *ApJ*, 891, 57
- Gavazzi, R., Treu, T., Koopmans, L. V. E., et al. 2008, *ApJ*, 677, 1046
- Jee, I., Suyu, S. H., Komatsu, E., et al. 2019, *Science*, 365, 1134
- Kessler, R., & Scolnic, D. 2017, *ApJ*, 836, 56
- Li, Y., Fan, X., & Gou, L. 2019, *ApJ*, 873, 37
- Li, Z., Ding, X., Wang, G.-J., Liao, K., & Zhu, Z.-H. 2018a, *ApJ*, 854, 146
- Li, Z.-X., Gao, H., Ding, X.-H., Wang, G.-J., & Zhang, B. 2018b, *Nature Communications*, 9, 3833
- Liao, K. 2019, *PhRvD*, 99, 083514
- Liao, K., Li, Z., Wang, G.-J., & Fan, X.-L. 2017, *ApJ*, 839, 70
- Liao, K., Shafieloo, A., Keeley, R. E., & Linder, E. V. 2019, *ApJL*, 886, L23
- , 2020, arXiv e-prints, arXiv:2002.10605
- Lin, H., Buckley-Geer, E., Agnello, A., et al. 2017, *ApJL*, 838, L15
- Lusso, E., & Risaliti, G. 2016, *ApJ*, 819, 154
- , 2017, *A&A*, 602, A79
- Marriner, J., Bernstein, J. P., Kessler, R., et al. 2011, *ApJ*, 740, 72
- Melia, F. 2019, *MNRAS*, 489, 517
- Pandey, S., Raveri, M., & Jain, B. 2019, arXiv e-prints, arXiv:1912.04325
- Peebles, P. J. E. 1993, *Principles of Physical Cosmology*
- Planck Collaboration, Aghanim, N., Akrami, Y., et al. 2018, arXiv e-prints, arXiv:1807.06209
- Qi, J., Cao, S., Biesiada, M., et al. 2019a, *PhRvD*, 100, 023530
- Qi, J.-Z., Cao, S., Zhang, S., et al. 2019b, *MNRAS*, 483, 1104
- Räsänen, S., Bolejko, K., & Finoguenov, A. 2015, *PhRvL*, 115, 101301
- Refsdal, S. 1964, *MNRAS*, 128, 307
- Riess, A. G., Casertano, S., Yuan, W., Macri, L. M., & Scolnic, D. 2019, *ApJ*, 876, 85
- Risaliti, G., & Lusso, E. 2015, *ApJ*, 815, 33
- , 2019, *Nature Astronomy*, 3, 272
- Rusu, C. E., Wong, K. C., Bonvin, V., et al. 2019, arXiv e-prints, arXiv:1905.09338
- Schneider, P., Ehlers, J., & Falco, E. E. 1992, *Gravitational Lenses*, doi:10.1007/978-3-662-03758-4
- Scolnic, D. M., Jones, D. O., Rest, A., et al. 2018, *ApJ*, 859, 101
- Shajib, A. J., Birrer, S., Treu, T., et al. 2020, *MNRAS*, arXiv:1910.06306
- Suyu, S. H., Marshall, P. J., Auger, M. W., et al. 2010, *ApJ*, 711, 201
- Suyu, S. H., Auger, M. W., Hilbert, S., et al. 2013, *ApJ*, 766, 70
- Suyu, S. H., Treu, T., Hilbert, S., et al. 2014, *ApJL*, 788, L35
- Verde, L., Treu, T., & Riess, A. G. 2019, *Nature Astronomy*, 3, 891
- Wong, K. C., Suyu, S. H., Auger, M. W., et al. 2017, *MNRAS*, 465, 4895
- Wong, K. C., Suyu, S. H., Chen, G. C. F., et al. 2019, arXiv e-prints, arXiv:1907.04869
- Xia, J.-Q., Yu, H., Wang, G.-J., et al. 2017, *ApJ*, 834, 75
- Yuan, W., Riess, A. G., Macri, L. M., Casertano, S., & Scolnic, D. M. 2019, *ApJ*, 886, 61
- Zhou, H., & Li, Z. 2020, *ApJ*, 889, 186